Better Catalysts through Microscopy: Mesoscale M1/M2 Intergrowth in Molybdenum–Vanadium Based Complex Oxide Catalysts for Propane Ammoxidation

Qian He,*,† Jungwon Woo,‡ Alexei Belianinov,§,∥ Vadim V. Guliants,*,‡ and Albina Y. Borisevich*,†,§

†Materials Science and Technology Division, Oak Ridge National Laboratory, Oak Ridge, Tennessee 37831, United States, ‡School of Energy, Environment, Biological and Medical Engineering, University of Cincinnati, Cincinnati, Ohio 45221-0012, United States, §Center for Nanophase Materials Sciences, Oak Ridge National Laboratory, Oak Ridge, Tennessee 37831, United States, and ∥Institute for Functional Imaging of Materials, Oak Ridge National Laboratory, Oak Ridge, Tennessee 37831, United States

ABSTRACT In recent decades, catalysis research has transformed from the predominantly empirical field to one where it is possible to control the catalytic properties *via* characterization and modification of the atomic-scale active centers. Many phenomena in catalysis, such as synergistic effect, however, transcend the atomic scale and also require the knowledge and control of the mesoscale structure of the specimen to harness. In this paper, we use our discovery of atomic-scale epitaxial interfaces in molybdenum–vanadium based complex oxide catalysts systems (*i.e.*, Mo–V–M–O, M = Ta, Te, Sb, Nb, *etc.*) to achieve control of the mesoscale structure of this complex mixture of very different active phases. We can now achieve true epitaxial intergrowth between the catalytically critical M1 and M2 phases in the system that are hypothesized to have synergistic interactions, and demonstrate that the resulting catalyst has improved selectivity in the initial studies. Finally, we highlight the crucial role atomic scale characterization and mesoscale structure control play in uncovering the complex underpinnings of the synergistic effect in catalysis.

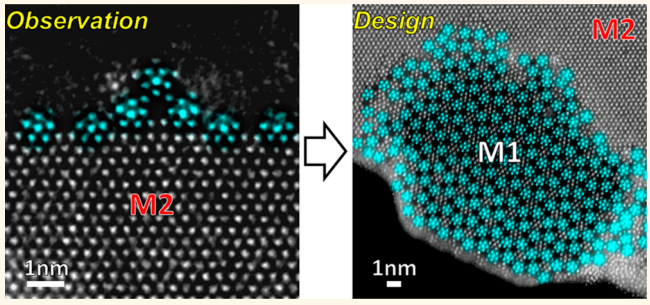

KEYWORDS: heterogeneous catalyst · aberration corrected STEM · propane ammoxidation · complex oxide

Synergistic effects, where multiple active components act collaboratively in chemical reactions for results greater than the sum of individual components acting alone, are commonly seen in catalysis. Classic examples include three-way catalysts for automobiles,[1] supported multimetallic nanoparticles,[2,3] *etc*. Exploiting the synergistic effect is therefore an important strategy for catalyst optimization, which usually demands control over the catalyst structure from individual active sites at atomic scale to the interaction among different active sites at mesoscale. Such level of control can be very difficult to attain for catalysts that are structurally complicated and have multiple active phases, such as Mo–V–M–O (M = Ta, Nb, Sb, Te) M1 and M2 mixed phase oxides. These complex oxides have recently drawn considerable research attention[4–6] as they are the most promising catalysts for propane ammoxidation reactions to make acrylonitrile (ACN), an industrially important chemical currently produced on a scale of 6 million tons annually.[7] The development of these oxide catalysts carries significant economic incentives, due to the possibility of replacing propylene with a much more abundant and inexpensive propane feedstock. Additionally, these catalysts have also shown promise for other selective oxidation reactions, such as propane oxidation[8–13] and ethane oxidative dehydrogenation.[14–18]

The synergistic effect between the M1 and the M2 phases in these oxides has been

* Address correspondence to heqian.lehigh@gmail.com, Vadim.Guliants@UC.EDU, albinab@ornl.gov.

Received for review November 25, 2014 and accepted March 6, 2015.

Published online March 06, 2015
10.1021/acsnano.5b00271

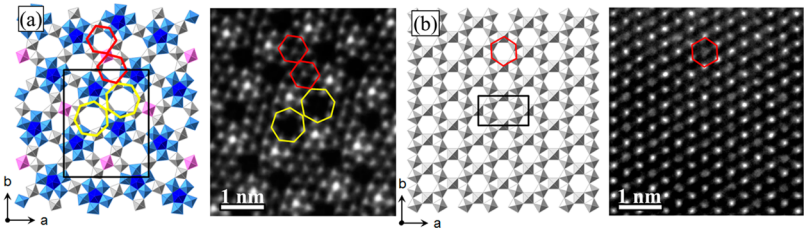

Figure 1. Polyhedral structural models and the representative HAADF images of (a) the M1 and (b) the M2 phases in Mo−V−Te−Ta oxide catalysts, viewed at the *ab*-plane. In the HAADF images, only cation columns are apparent as oxygen has a lower atomic number and is not visible due to dynamic range issues. Black frames in the models represent the unit cells in each structure M_6O_{21} type (M = Ta, Mo or V) units in the M1 phase are highlighted as follows: MO_7 pentagonal bipyramids are highlighted in dark blue and surrounded by edge sharing light blue MO_6 octahedra; gray squares represent the rest of the connecting MO_6 octahedra. The polyhedral network has resulted in heptagonal (M1 phase only, shown in yellow) and hexagonal channels (M1 and M2 phases, highlighted in red). The visibility of Te oxide units inside these channels depend on their occupancies. Te oxide units in the channels are omitted in the structural model in order to make the framework structure clearer.

proposed as one of the key reasons for high catalytic performance, observed in the M1+M2 mixtures obtained either by mechanical mixing[19] or one pot cosynthesis method.[5] The "M1" and "M2" phase names were originally coined for the two critical phases in the Mo−V−Te−Nb oxide catalysts developed by Mitsubishi Chemical Corporation[20−23] and later adopted as a shorthand reference for related isostructural compounds with a range of stoichiometries. Typical formulas of the M1 and the M2 phase for Mo−V−Te−Nb system are $Mo_{7.8}V_{1.2}NbTe_{0.937}O_{28.9}$ and $Mo_{4.31}V_{1.36}Te_{1.81}Nb_{0.33}O_{19.81}$, respectively.[24] In terms of crystal structure, the two phases are very different:[24] The M1 phase (ICSD no. 55097) has a layered orthorhombic structure, with layers made up of networks of M_6O_{21} type units (composed of a central MO_7 pentagonal bipyramid, sharing edge with 5 surrounding MO_6 octahedra), forming heptagonal and hexagonal channels each in a doublet fashion (Figure 1a). In contrast, the pseudohexagonal M2 phase (ICSD no. 55098) does not have any M_6O_{21} type units, and instead has a layered structure with corner sharing MoO_6 octahedra, forming hexagonal channels only (Figure 1b). Catalytically, the M1 phase alone was found to be active and selective in the propane (amm)oxidation reactions, while the pure M2 phase was not able to activate propane.[10,11,25,26] Nevertheless, the best reported catalysts still contain significant amount of the M2 phase (about 40 wt % in the Mo−V−Te−Nb oxide system).[27] The reason behind this is unclear. On one hand,[28] the M2 phase is believed to be more efficient and selective in converting the propylene intermediate into final products, thus explaining higher reaction selectivity seen when both phases are present. On the other hand, Baca *et al.*[29] suggested that the synergistic effect happens because the M2 phase replenishes key elements lost from the M1 phase during the reaction, thus preventing its deactivation, as they found the synergistic effect only in the Te containing systems. To complicate matters further, the very existence of the synergistic effect has been brought into question, by Korovchenko *et al.*;[30,31] who showed that the M1+M2 mixture can produce higher ACN selectivity in the low and medium conversion condition in the propane ammoxidation reaction, but at higher conversion condition, M1 phase alone performs the best.

This ambiguity stems from the lack of control over mixing of the M1 and M2 phases at mesoscale, as no attempt is made to ensure the M1 and the M2 phases interact similarly in different experiments. These complex oxides are normally prepared using wet-chemistry synthesis with precise requirements for conditions such as temperature and pH to ensure the formation of the desired phases. Typically, as-synthesized powders consist of micrometer or submicrometer[32] sized rod-shaped or platelet-like crystals, thus making the phase interactions relatively long-range as well as strongly dependent on specific microstructure of the sample. Nanometer scale M1 and M2 phase mixing was speculated to occur in catalysts prepared *via* one-pot cosynthesis;[27] however, no such evidence has ever been found.[33] Creating a material with nanometer scale mixing of the M1 and the M2 will help develop fundamental understanding of the synergistic effect in this system and bring opportunities for further catalyst design and optimization.

RESULTS AND DISCUSSIONS

Surface Decoration of "M1-like" M_6O_{21} Type Units on the M2 Phase. While performing an aberration corrected STEM study on a series of Mo−V−M catalysts, we have uncovered evidence for spontaneously forming M1/M2 epitaxial interface. Figure 2 shows representative STEM-HAADF images of a Mo−V−Te−Ta oxide catalyst sample (catalyst (A)) synthesized with a lower [Te]/[Ta] ratio of 8/27, resulting in preferential formation of the M2 phase. The particle is viewed from the [001] zone axis, displaying the projection of the *a*−*b* plane. As shown in Figure 2a, while the interior of the particle is found to be the expected M2 phase, the side facets appear to be decorated with a distinctive layer of M_6O_{21} type units. The surface decorations are found in all M2 phase particle examined and on all type of side

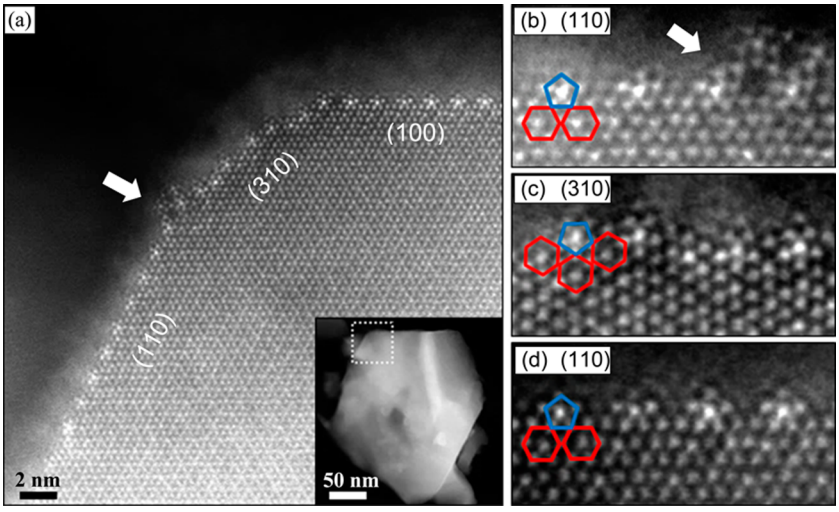

Figure 2. Representative STEM-HAADF images showing Mo_6O_{21} type units decorating the side planes of M2 phase particles in the catalyst (A), which is Mo−V−Te−Ta oxide prepared with a *lower* [Te]/[Ta] ratio. (a) STEM-HAADF image of a M2 phase particle viewed along the [001] axis. The inset is the lower magnification STEM-HAADF image showing the overview of the particle. Magnified view of the "M1-like" Mo_6O_{21} type units on (110), (310), and (100) facet are shown in (b), (c), and (d), respectively. Mo_6O_{21} type units are found in all types of facets. The blue pentagons and red hexagons highlighted in the HAADF image demonstrate the type I interface between the M_6O_{21} type units with the M2 phase (pentagons and hexagons are sharing vertexes, each of which represents a MO_6 octahedron). In most cases, the coverage of Mo_6O_{21} type units appears to be monolayer. The white arrow highlights the region where pentagonal unit decoration goes beyond monolayer so that a heptagonal channel was formed. The widths of images (b), (c), and (d) are about 6 nm.

facets, including both "arm-chair"-like (001), (110) and "zigzag"-like (310) (Supporting Information Figure S1). In all three cases shown in Figure 2b−d, epitaxial interfaces are formed in such a way that M_6O_{21} type units (highlighted as blue pentagons) are sharing MO_6 octahedra with the M2 phase hexagonal rings (highlighted as red hexagons). We call this kind of interface "type I". Another interesting finding is that the cation column in the central bipyramidal site of the M_6O_{21} type units appears to have much higher HAADF intensity than the surrounding ones (Supporting Information Figure S2a). Although quantitative analysis based on model based frozen phonon calculation[34,35] is not available due to the lack of precise knowledge of the interface structure, composition, and thermal parameters (*i.e.*, Debye−Waller factor), qualitative intensity comparison strongly suggested the enrichment of Ta on the central bipyramidal site, which is consistent with the previously reported preference of pentavalent elements (*i.e.*, Ta, Nb) for occupying these sites.[34] In addition, although the majority of M_6O_{21} type units form just one layer, occasionally a fully formed heptagonal channel can be found (Figure 2b white arrow), indicating that multiple layers of M_6O_{21} type units on M2 surface are possible.

To the best of our knowledge, this is the first observation of the epitaxial interface between Mo_6O_{21} type units with the M2 phase matrix in the Mo−V−M catalyst system. Our observations show that "M1-like" Mo_6O_{21} type units (a) cover all types of side facets of the M2 phase, (b) are compositionally distinct (likely Ta enriched in the bipyramidal sites) from the M2 phase matrix, and (c) can grow beyond one monolayer. These suggest that the M1/M2 epitaxial intergrowth might be possible, provided that the formation mechanism of the observed surface decoration of Mo_6O_{21} type units can be understood and harnessed. Is it a surface reconstruction behavior of the M2 phase? Is it an intermediate growth step of the M2 phase? Or is it a true intergrowth that can lead to M1/M2 heterostructure?

Understanding the Formation Mechanism. Ueda and others[8,36,37] proposed that for Mo−V based oxides, the formation of various crystal structures follows a building-block self-assembly mechanism. Their *in situ* Raman and UV−vis studies found that $Mo_{72}V_{30}$ polyoxomolybdate molecules that contain Mo_6O_{21} type units need to be present in the precursor solution in order to synthesize structures with orthorhombic phase or trigonal phase, both of which have Mo_6O_{21} type units as building blocks. Following their work, we propose that the Mo−V−Te−Ta oxide adopts a similar mechanism: $TaMo_5O_{21}$ type units are stabilized by the presence of pentavalent element Ta in the precursor solution; these units later self-assemble onto the pre- or simultaneously formed M2 phase particle surface.

To test this hypothesis, we carried out additional experiments: First, we synthesized two additional M2 phase catalysts without Ta, namely Mo−V−Te oxide and Mo−V−Te−Nb oxide, using a slurry evaporation protocol. The HAADF-STEM images of these catalysts are shown in Supporting Information Figure S3a,b. No surface decoration of M_6O_{21} type units on the M2 phase particles was found in these two catalysts. In

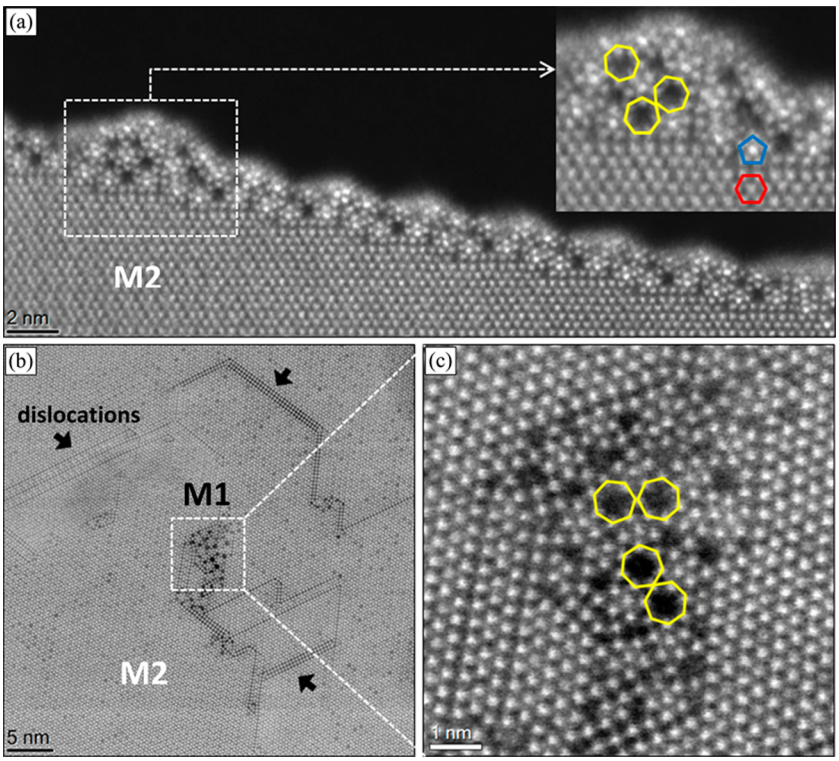

Figure 3. Representative STEM-HAADF images of the Mo−V−Sb−Ta oxide M2 phase catalyst. (a) The surface of the M2 phase particle is covered by multiple layers of M_6O_{21} type units. The type II interface is highlighted by a blue pentagon (M_6O_{21} type unit) and a red hexagon (a hexagonal ring in the M2 phase). They are separated instead of sharing corners as in the case of the type I interface, indicating that the MO_6 type octahedra in M_6O_{21} type units are sharing corner oxygen atoms with those in the M2 hexagonal rings. The inset shows a doublet heptagonal channels (highlighted in yellow) formed in the surface layer. (b and c) the M1 phase (doublet heptagonal channels highlighted in yellow) formed inside the M2 phase particle. The materials surrounding the M1 phase appear to be very defective. Additional defects such as dislocations are also found in the surrounding M2 phase (black arrows).

the Mo−V−Te−Nb oxide system, other phases that contain M_6O_{21} type units (Supporting Information Figure S3c,d) were occasionally found.

These results suggest that the observed epitaxial growth of M_6O_{21} type units is strongly associated with the presence of Ta in the system. In the case of Mo−V−Te oxide, we can infer that the M_6O_{21} type units were probably not stable in our synthesis conditions. The scenario is different for the Mo−V−Te−Nb system, as Nb, another pentavalent element, is known to have a similar stabilizing effect on the M1 phase as compared to Ta.[27] It appears that those presumably $NbMo_5O_{21}$ type units are "consumed" in forming separate particles of other phases, instead of epitaxially assembling on the M2 phase. Clearly, having M_6O_{21} type building blocks is not a sufficient condition for the observed heterostructure to form. One possible explanation is that the self-nucleation of impurity phases is energetically more favorable than interface formation for $NbMo_5O_{21}$ type units in our synthesis conditions. Future *in situ* studies[36] are required to get more insight into the dynamic process of the crystal growth in these systems.

Nevertheless, the epitaxial growth of M_6O_{21} type units on the M2 phase surface is a robust behavior for Ta containing systems. Representative STEM-HAADF images of another Ta containing Mo−V−Sb−Ta oxide M2 phase catalyst are shown in Figure 3. Surface decoration of M_6O_{21} type units on the M2 phase particles is clearly present, and in this case the growth of M_6O_{21} type units develops well beyond monolayer coverage. Interestingly, we found another type of interface (henceforth referred to as "type II") between M_6O_{21} type units and the hexagonal rings of the M2 phase, where the contacting MO_6 octahedra are sharing corner oxygen atoms. More importantly, "doublet" heptagonal channels have been found (highlighted in yellow in Figure 3(a)), suggesting full formation of the M1 phase. Additionally, as shown in Figure 3b,c, there are areas within the M2 phase matrix where M1 phase structure can be found. Surrounding the M1 phase there appear to be structural defects that could counteract the lattice mismatch between the two phases. Such distortions might be further balanced by the nearby dislocations found in the M2 phase matrix (black arrows in Figure 3b).

The findings about strong association with Ta, the multilayer growth and the inclusion formation of M_6O_{21} type units in the Mo−V−Sb−Ta system all point to a self-assembly process as opposed to the hypotheses about surface reconstruction and intermediate growth state of M2. We therefore summarize our

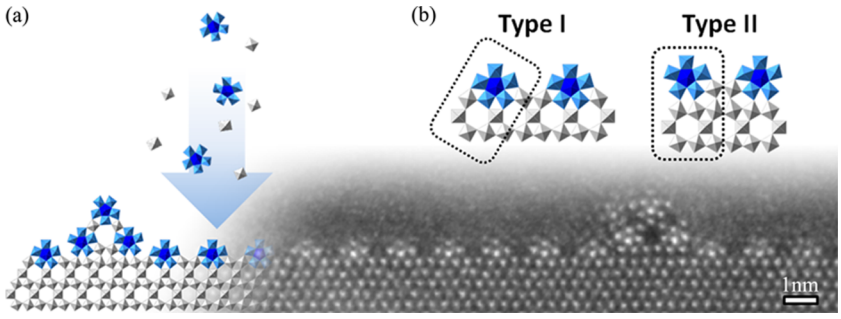

Figure 4. (a) STEM-HAADF image and polyhedral schematic demonstrating the proposed formation mechanism of the observed heterostructure between "M1-like" $TaMo_5O_{21}$ type units with the M2 phase. $TaMo_5O_{21}$ type units were preformed in the solution and epitaxially attached to the surface of the M2 phase to form interfaces (both type I and type II, as shown in (b), highlighted by black dash lines) during the self-assembly process. The bottom right part shows the STEM-HAADF image of the surface of a M2 phase particle in the Mo−V−Te−Ta oxide prepared with lower [Ta]/[Te] ratio, viewed along the [001] zone axis. The left side shows the corresponding polyhedral structural model of the interface between "M1-like" M_6O_{21} type units (blue) with the M2 phase (gray). Te oxide units in the channels are omitted in the structural model for clarity.

proposed formation mechanism in Figure 4. We have identified two necessary requirements for the "M1-like" M_6O_{21} type units to form an interface with the M2 phase: (1) availability of M_6O_{21} type units in the precursor solution; (2) thermodynamic and kinetic preference for the interface formation *versus* self-nucleation of other phases. Because of the highly dynamical nature of the crystal growth process, we cannot rule out the possibility of similar phenomenon happening in other systems unless we also tune the synthesis conditions. Additional work is needed to uncover the details of the self-assembly process. For instance, one interesting question to ask is why surface decoration of the M_6O_{21} type units is much more common than the inclusions. Is it because the M2 phase grows much faster or because the M_6O_{21} type units only form in the reaction environment after the initial composition has been altered by the M2 phase formation?

Synthesizing M1/M2 Intergrown Heterostructure Catalyst. The preliminary understanding of the mechanism enables us to explore the possibility of larger intergrowth between the M1 and the M2 phases. Since we propose that the M1 phase comes from the $TaMo_5O_{21}$ type units, bigger M1 phase intergrowth will require a larger "supply" of the $TaMo_5O_{21}$ type units during the synthesis. To test this suggestion, we synthesized another Mo−V−Te−Ta oxide catalyst with higher [Ta]/[Te] ratio of 12:17 (catalyst (B)). The resultant catalyst was an approximately 1:1 mixture of the M1 and the M2 phases determined by XRD (Supporting Information Figure S4). In this catalyst, M2 phase particles (Figure 5), as well as isolated M1 phase particles (Supporting Information Figure S5), are present. A closer look at the M2 phase particle (Figure 5b−d) reveals that (a) the side facets of the M2 phase particles are still covered with M_6O_{21} type units, and their center bipyramidal sites have higher intensity than surrounding columns, signifying preferential Ta occupation; (b) at some locations we can find full M1/M2 phase intergrowth with continuous M1 regions (tens of nm in size) coherently coupled with M2 regions (Figure 5c,d). Interestingly, in some cases the [001] zone of the intergrown M1 phase is aligned with the [001] zone of the M2 matrix so that we can resolve the lattice for both structures simultaneously (Figure 5c), but in other cases, they are not aligned, suggesting additional types of M1/M2 interfaces beyond the type I and II interfaces shown in Figure 4 (*i.e.*, M1' grain in Figure 5d). An additional example of such intergrowth is shown in Supporting Information Figure S6, where the M1 and the M2 phases can be tilted to zone axis separately.

Epitaxial intergrowth between the M1 and the M2 phase in the Mo−V−Te−Ta oxide catalyst system is thus achieved, indicating that mixing these two catalytically important phases at the nanometer scale is feasible. Note that a significant amount of isolated M1 phase particles was formed, suggesting that self-nucleation was also taking place. This phenomenon could be due to a higher concentration of pentagonal units in the precursor solution, either globally, or locally as a result of mass transfer fluctuation during synthesis. Interestingly, the enhanced M1 phase intergrowth is not uniformly distributed on the M2, unlike the surface decoration of the "M1-like" M_6O_{21} type units in the original "M2-phase" sample. A more refined synthesis approach might enable us to maximize the population of these interfaces, or possibly achieve the intergrowth for Ta-free systems, such as the most active Mo−V−Te−Nb system, by using seeded growth of M1 phases on the Ta−pentagon decorated M2 phase particles.

We then carried out catalytic property measurements of the intergrown M1/M2 in propane ammoxidation reactions on three selected catalysts. In addition to the previously described catalyst (A) (M2 phase with surface decoration of M_6O_{21} type units) and catalyst (B) (10s nm scale M1 phase grown on the M2 phase, also with isolated M1 phase particles), the catalyst (C) is prepared by treating catalyst (B) with H_2O_2[38] in order to selectively dissolve the M2 phase

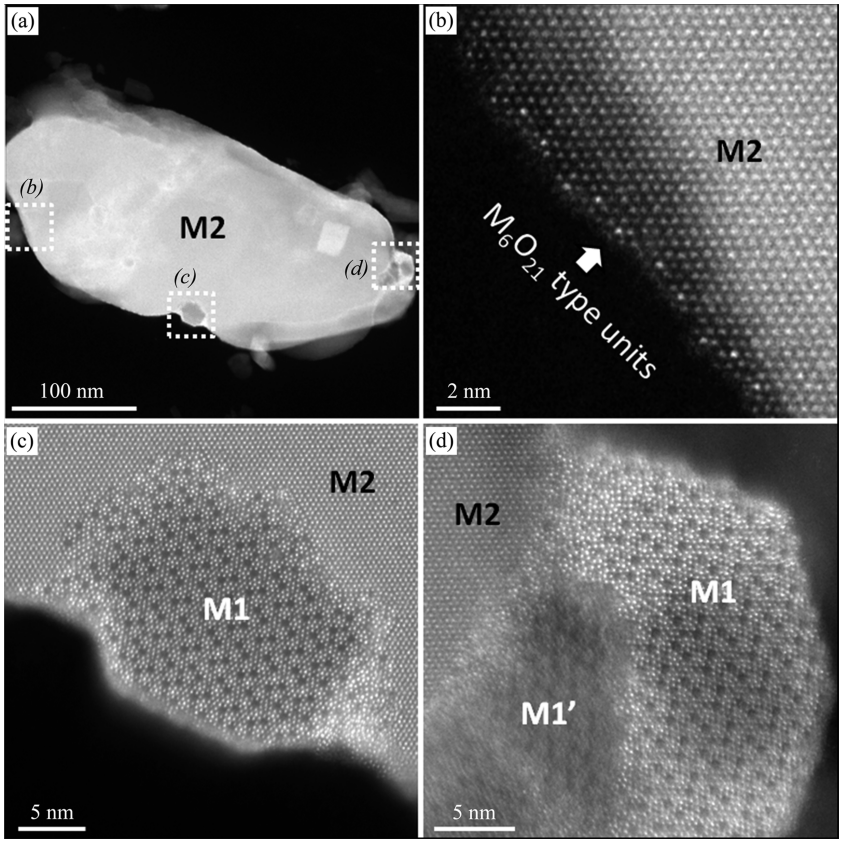

Figure 5. Representative STEM-HAADF images of the catalyst (B), a Mo–V–Te–Ta oxide prepared with a *higher* [Ta]/[Te] ratio, viewed along the [001] projection. (a) Lower magnification HAADF image showing the overview of the M2 phase particle. Areas highlighted in white are shown in (b–d). (b) Magnified view of the side facet of the M2 phase particle, which is decorated with M_6O_{21} type units. Their center bipyramidal sites have higher intensity than surrounding columns, signifying preferential Ta occupation. (c and d) Magnified view of the area where full M1 phase has developed on the M2 phase particle. The [001] axis of M1 and M2 phase can be parallel to each other so we can visualize the lattice for both phase simultaneously. However, this is not always the case as some M1 phase grains (*i.e.*, marked M1′ in (d)) can have different orientations.

TABLE 1. Catalytic Measurement Results for Propane Ammoxidation Reaction on Several Mo–V–Te–Ta Oxide Catalysts at Low and Medium Conversion Conditions[a]

			selectivity (%)			
catalyst sample	*T* (°C)	conversion (%)	acrylonitrile	propylene	acetonitrile	CO_x
(A) **M2**	380	0	N/A	N/A	N/A	N/A
(B) **M1/M2**	380	4.7	49.5	49	1.4	0
(C) **M1**	380	2.9	9.2	87.2	3.6	0
(A) **M2**	420	0	N/A	N/A	N/A	N/A
(B) **M1/M2**	420	47.8	65.1	4	3.2	27.3
(C) **M1**	420	45.7	50	4.4	3.3	42.2

[a] Reaction condition—feed composition: $C_3H_8/NH_3/O_2/He = 5.7:8.6:17.1:68.6$ (%); contact time *W*/*F*, 0.0083–0.1449 gcat · min/mL.

particles and thus pure M1 phase is achieved. The propane ammoxidation reaction was carried out using previously reported[38] protocols at the temperatures of 380 and 420 °C, in order to obtain different levels of propane conversion. The catalytic testing results are shown in Table 1. The catalyst (A) was not able to activate propane at either temperature, giving zero conversion. The catalyst (C) gives a conversion of 2.9% and acrylonitrile selectivity of 9.2% at 380 °C, and a conversion of 45.7% with an acrylonitrile selectivity of 50% at 420 °C. The catalyst (B) gives significantly higher acrylonitrile selectivity at both reaction temperatures: 49.5% at 380 °C and 65.1% at 420 °C, along with a propane conversion of 4.7% and 47.8% respectively.

The catalytic testing results suggest that, first, the surface pentagonal decoration on the M2 phase particles in catalyst (A) does not provide active sites for propane activation. The identity of the propane activation sites in the M1 phase catalyst were believed by some to be located on the (001) basal plane of the crystal structure,[4,27,28,39] while others suggested that the side planes can also be active.[10,25] This catalyst (A) provided a rare example where the side planes of the catalyst particle largely appear to be "M1-like", while the basal planes remain to be the M2 phase. Lack of catalytic activity strongly supports the hypothesis that the basal plane of the M1 phase is crucial.

Second, the catalyst (B) with M1/M2 intergrowth has significantly higher acrylonitrile selectivity compared to pure M1 phase catalyst (C), suggesting a major synergistic effect is in play for the catalyst (B). The

presence of isolated M1 phase will also contribute to the overall synergy thus preventing a quantitative evaluation of the effect arising from having M1/M2 interfaces. Given what we now know about complex structural and chemical relations between the phases in this system, a conclusive answer to this question and the eventual design of the ultimate propane (amm)oxidation catalyst will require a new approach to synthesis and testing. Some previously reported data on catalytic activity measurements likely contains contributions from structural features found in this work that are not taken into account for the mechanism discussions. We are currently developing advanced testing protocols that explicitly control for the contributions from surface area, extent of intergrowth, and nanoscale phase composition.

Last but not least, along with the synergistic effect that may arise from the improved M1 and M2 phase proximity, the M1/M2 interface itself, with its unprecedented arrangements of cations, can have an effect on catalytic activity. We have shown that multiple types of interfaces between the M1 and the M2 phases are possible. In addition, the recently developed local configuration analysis (LCA)[40] was used to classify local atomic environments of cation columns in the intergrown particles. As shown in Supporting Information Figure S7, some cations at the interface between M1 and M2 phases have atomic environments (labeled in yellow in Supporting Information Figure S7) different from those in either M2 (green) or M1 (magenta) phases, which is likely to result in different catalytic properties.

In summary, aberration corrected STEM has been used to help design a synthesis route for an improved catalyst by achieving mesoscale control of the intergrowth of two catalytically important phases. We first discovered that "M1-like" M_6O_{21} type units are spontaneously decorating the side facets of the M2 phase, forming epitaxial interfaces and some M1-phase regions of subunit-cell size in the Ta-containing Mo−V−M oxide catalysts. The formation mechanism of such structure was proposed to follow a self-assembly process, activated when M_6O_{21} type units are stabilized in the precursor solutions and interface formation is energetically favorable over isolated nucleation. We then exploit this mechanism to successfully modify our synthesis approach, resulting in enhanced intergrowth of the M1 and the M2 phases, with coherent M1 phase regions tens of nanometers in size. We also identified that the M_6O_{21} type units in the M1 phase form different types of interfaces with the M2 phases (type I and II when [001] axes are aligned, and additional types with [001] axes are not aligned). We believe this work proves that controlling the mixing of these two catalytically important phases at the nanometer scale is possible, opening completely new avenues to improve their catalytic performance. Since the above findings are done on the samples prepared by standard protocols with varying composition, it is highly possible that such intergrowth might already exist, unnoticed, in many classic works in this field. We hope that new synthesis approaches are developed to achieve multilayer M1/M2/M1... heterostructure. Additionally, the current work provides important evidence for the long debated significance of the basal plane of the M1 phase for propane activation, as the M2 phase particle decorated with building blocks of the M1 phase was found inactive. Finally, this work has also shown that comprehensive atomic scale structural and chemical characterization by aberration corrected STEM can lead to understanding and control of the atomic and mesoscale structure in complex catalyst systems.

EXPERIMENTAL METHODS

Material. The Mo−V−M oxides were prepared by hydrothermal synthesis (HT) or slurry evaporation (SE) as previously reported.[41,42] Ammonium paramolybdate, telluric acid, antimony trioxide, vanadium(IV) sulfate, niobium(V) oxalate hexahydrate and tantalum(V) ethoxide were used as precursors. All operations, preparation and stirring of the solution, were performed at 353 K except Sb system at 373 K. The slurry was introduced into the Teflon inner tube of a stainless steel autoclave. In the case of slurry evaporation, this slurry was dried overnight in the oven at 383 K. The autoclave was sealed and heated at 448 K for 48 h. After hydrothermal synthesis, the dark blue powder obtained was washed, filtered with distilled water (200 mL) and dried at 353 K overnight. Then, the dried powder catalyst was calcined under ultra-high purified nitrogen flow (50 mL/min) at 873 for 2 h before use. In the case of catalyst containing Sb, the obtained solid was preheated in furnace with air at 573 K for 4 h before it was calcined under ultra-high purified nitrogen flow at 873 for 2 h. The nominal compositions (molar ratio) of the catalysts involved in the work are as follows: for Mo−V−Te−Ta oxide with lower [Ta]/[Te] ratio, Mo/V/Te/Ta = 1:0.31:0.27:0.08; for Mo−V−Te−Ta oxide with higher [Ta]/[Te] ratio, Mo/V/Te/Ta = 1:0.3:0.17:0.12; for Mo−V−Te oxide, Mo/V/Te = 1:0.75:0.75 ; for Mo−V−Te−Nb oxide, Mo/V/Te/Nb = 1:0.31:0.27:0.08; for Mo−V−Sb−Ta oxide, Mo/V/Sb/Ta = 1:0.3:0.3:0.1.

Electron Microscopy. To make specimen for electron microscopy, the catalyst sample was embedded in a resin, and sectioned by microtome as approximately 50 nm slices.[34] These specimens were introduced into a holey carbon coated Cu grid. The HAADF-STEM imaging was performed on Nion UltraSTEM 100 (operated at 100 kV) and UltraSTEM 200 (operated at 200 kV) at Oak Ridge National Laboratory.

X-ray Diffraction (XRD). The powder X-ray diffraction patterns were recorded by a Siemens D500 diffractometer using Cu Kα radiation (tube voltage, 45 kV; tube current, 40 mA). Pure Mo−V−Te−Ta−O M1 phase, pure M2 phase and three mixtures containing different weight fractions of pure M1 and M2 phases (M1/M2 ratios of 1:3, 1:1, and 3:1) were characterized by XRD and the characteristic peak areas at $2\Theta = 27.1°$ for the M1 phase and $2\Theta = 36.1°$ for the M2 phase[29] were determined using PANalytical X'Pert HighScore software. The calibration curve

thus obtained was employed to determine the M1/M2 phase content in all catalysts.

Catalytic Property Testing. The catalytic properties of Mo−V−Te−Ta oxides were tested in propane ammoxidation using a fixed bed microreactor equipped with an on-line GC under steady-state conditions at atmospheric pressure and 380−420 °C. Powder sample after calcination was ground with mortar and pestle for 5 min and diluted with quartz sand prior to the catalyst testing. The diluted catalysts were introduced into the microreactor, heated to the desired temperatures under He flow and exposed to the reaction feed. The feed was composed of C_3H_8 (C_3H_8)/NH_3/O_2/He in the molar ratio of 6(6):7:17:70 (the total flow rate of 24 mL·min^{-1}). The reactants and products were analyzed by an on-line GC system (Shimadzu 14 A) equipped with a flame ionization detector and a thermal conductivity detector. The total carbon balances agreed within ±5%.

Conflict of Interest: The authors declare no competing financial interest.

Supporting Information Available: The polyhedral model of the M2 phase showing two types of facets, additional STEM-HAADF images mentioned in the main text, XRD results and the Local configuration analysis (LCA) result are shown in Figures S1−S7. This material is available free of charge *via* the Internet at http://pubs.acs.org.

Acknowledgment. Electron microscopy research (Q.H. and A.Y.B.) is supported by the U.S. Department of Energy, Office of Science, Basic Energy Sciences, Materials Sciences and Engineering Division and through a user project supported by ORNL's Center for Nanophase Materials Sciences, sponsored by the Scientific User Facilities Division, Office of Science, Basic Energy Sciences, U.S. Department of Energy. Catalyst synthesis and testing (J.W. and V.V.G.) is supported by Chemical Sciences, Geosciences and Biosciences Division, Office of Science, Basic Energy Sciences, U.S. Department of Energy, under Grant #DE-FG02-04ER15604. LCA analysis (A.B.) was conducted at the Center for Nanophase Materials Sciences, which is sponsored at Oak Ridge National Laboratory by the Scientific User Facilities Division, Office of Science, Basic Energy Sciences, U.S. Department of Energy.

REFERENCES AND NOTES

1. Fu, W.; Li, X. H.; Bao, H. L.; Wang, K. X.; Wei, X.; Cai, Y. Y.; Chen, J. S. Synergistic Effect of Bronsted Acid and Platinum on Purification of Automobile Exhaust Gases. *Sci. Rep.* **2013**, *3*, 2349.
2. Holewinski, A.; Idrobo, J.-C.; Linic, S. High-Performance Ag−Co Alloy Catalysts for Electrochemical Oxygen Reduction. *Nat. Chem.* **2014**, *6*, 828–834.
3. Enache, D. I.; Edwards, J. K.; Landon, P.; Solsona-Espriu, B.; Carley, A. F.; Herzing, A. A.; Watanabe, M.; Kiely, C. J.; Knight, D. W.; Hutchings, G. J. Solvent-free Oxidation of Primary Alcohols to Aldehydes Using Au-Pd/TiO_2 Catalysts. *Science* **2006**, *311*, 362–5.
4. Shiju, N. R.; Guliants, V. V. Recent Developments in Catalysis Using Nanostructured Materials. *Appl. Catal., A* **2009**, *356*, 1–17.
5. Grasselli, R. K.; Buttrey, D. J.; Burrington, J. D.; Andersson, A.; Holmberg, J.; Ueda, W.; Kubo, J.; Lugmair, C. G.; Volpe, A. F. Active Centers, Catalytic Behavior, Symbiosis and Redox Properties of MoV(Nb,Ta)TeO Ammoxidation Catalysts. *Top. Catal.* **2006**, *38*, 7–16.
6. DeSanto, P.; Buttrey, D. J.; Grasselli, R. K.; Lugmair, C. G.; Volpe, A. F.; Toby, B. H.; Vogt, T. Structural Characterization of the Orthorhombic Phase M1 in MoVNbTeO Propane Ammoxidation Catalyst. *Top. Catal.* **2003**, *23*, 23–38.
7. Brazdil, J. F., Acrylonitrile. In *Ullmann's Encyclopedia of Industrial Chemistry*; Wiley-VCH Verlag GmbH & Co. KGaA: Weinheim, Germany, 2012.
8. Ueda, W. Establishment of Crystalline Complex Mo-V-Oxides as Selective Oxidation Catalysts. *J. Jpn. Pet. Inst.* **2013**, *56*, 122–132.
9. Heine, C.; Havecker, M.; Sanchez-Sanchez, M.; Trunschke, A.; Schlogl, R.; Eichelbaum, M. Work Function, Band Bending, and Microwave Conductivity Studies on the Selective Alkane Oxidation Catalyst MoVTeNb Oxide (Orthorhombic M1 Phase) under Operation Conditions. *J. Phys. Chem. C* **2013**, *117*, 26988–26997.
10. Schlogl, R. Active Sites for Propane Oxidation: Some Generic Considerations. *Top. Catal.* **2011**, *54*, 627–638.
11. Sanfiz, A. C.; Hansen, T. W.; Teschner, D.; Schnorch, P.; Girgsdies, F.; Trunschke, A.; Schlogl, R.; Looi, M. H.; Hamid, S. B. A. Dynamics of the MoVTeNb Oxide M1 Phase in Propane Oxidation. *J. Phys. Chem. C* **2010**, *114*, 1912–1921.
12. Grasselli, R. K.; Lugmair, C. G.; Volpe, A. F.; Andersson, A.; Burrington, J. D. Inhibition of Propylene Oxidation to Acrylic Acid by Amorphous Overlayers on MoV(Nb)TeO Based M2 Catalysts. *Catal. Lett.* **2008**, *126*, 231–240.
13. Vitry, D.; Morikawa, Y.; Dubois, J. L.; Ueda, W. Propane Selective Oxidation over Monophasic Mo-V-Te-O Catalysts Prepared by Hydrothermal Synthesis. *Top. Catal.* **2003**, *23*, 47–53.
14. Valente, J. S.; Armendáriz-Herrera, H.; Quintana-Solórzano, R.; del Ángel, P.; Nava, N.; Massó, A.; López Nieto, J. M. Chemical, Structural, and Morphological Changes of a MoVTeNb Catalyst during Oxidative Dehydrogenation of Ethane. *ACS Catal.* **2014**, *4*, 1292–1301.
15. Ishikawa, S.; Murayama, T.; Ohmura, S.; Sadakane, M.; Ueda, W. Synthesis of Novel Orthorhombic Mo and V Based Complex Oxides Coordinating Alkylammonium Cation in Its Heptagonal Channel and Their Application as a Catalyst. *Chem. Mater.* **2013**, *25*, 2211–2219.
16. Konya, T.; Katou, T.; Murayama, T.; Ishikawa, S.; Sadakane, M.; Buttrey, D.; Ueda, W. An Orthorhombic Mo3VOx Catalyst Most Active for Oxidative Dehydrogenation of Ethane Among Related Complex Metal Oxides. *Catal. Sci. Technol.* **2013**, *3*, 380–387.
17. Nguyen, T. T.; Burel, L.; Nguyen, D. L.; Pham-Huu, C.; Millet, J. M. M. Catalytic Performance of MoVTeNbO Catalyst Supported on SiC Foam in Oxidative Dehydrogenation of Ethane and Ammoxidation of Propane. *Appl. Catal., A* **2012**, *433*, 41–48.
18. Nguyen, T. T.; Aouine, M.; Millet, J. M. M. Optimizing the Efficiency of MoVTeNbO Catalysts for Ethane Oxidative Dehydrogenation to Ethylene. *Catal. Commun.* **2012**, *21*, 22–26.
19. Holmberg, J.; Grasselli, R. K.; Andersson, A. Catalytic Behaviour of M1, M2, and M1/M2 Physical Mixtures of the Mo−V−Nb−Te−oxide System in Propane and Propene Ammoxidation. *Appl. Catal., A* **2004**, *270*, 121–134.
20. Ushikubo, T. Recent Topics of Research and Development of Catalysis by Niobium and Tantalum Oxides. *Catal. Today* **2000**, *57*, 331–338.
21. Ushikubo, T.; Oshima, K.; Numazawa, T.; Vaarkamp, M.; Sawaki, I. Ammoxidation of Propane over Mo-V-Nb-Te Mixed Metal Oxide Catalysts. *Stud. Surf. Sci. Catal.* **1999**, *121*, 339–342.
22. Ushikubo, T.; Oshima, K.; Kayou, A.; Vaarkamp, M.; Hatano, M. Ammoxidation of Propane over Catalysts Comprising Mixed Oxides of Mo and V. *J. Catal.* **1997**, *169*, 394–396.
23. Ushikubo, T.; Oshima, K.; Kayou, A.; Hatano, M. Ammoxidation of Propane over Mo-V-Nb-Te Mixed Oxide Catalysts. *Stud. Surf. Sci. Catal.* **1997**, *112*, 473–480.
24. DeSanto, P.; Buttrey, D. J.; Grasselli, R. K.; Lugmair, C. G.; Volpe, A. F.; Toby, B. H.; Vogt, T. Structural Aspects of the M1 and M2 Phases in MoVNbTeO Propane Ammomidation catalysts. *Z. Kristallogr.* **2004**, *219*, 152–165.
25. Amakawa, K.; Kolen'ko, Y. V.; Villa, A.; Schuster, M. E.; Csepei, L. I.; Weinberg, G.; Wrabetz, S.; d'Alnoncourt, R. N.; Girgsdies, F.; Prati, L.; Schlogl, R.; Trunschke, A. Multifunctionality of Crystalline MoV(TeNb) M1 Oxide Catalysts in Selective Oxidation of Propane and Benzyl Alcohol. *ACS Catal.* **2013**, *3*, 1103–1113.
26. Muthukumar, K.; Yu, J. J.; Xu, Y.; Guliants, V. V. Propane Ammoxidation Over the Mo-V-Te-Nb-O M1 Phase: Reactivity of Surface Cations in Hydrogen Abstraction Steps. *Top. Catal.* **2011**, *54*, 605–613.

27. Grasselli, R. K.; Burrington, J. D.; Buttrey, D. J.; DeSanto, P.; Lugmair, C. G.; Volpe, A. F.; Weingand, T. Multifunctionality of Active Centers in (Amm)oxidation Catalysts: from Bi-Mo-O-x to Mo-V-Nb-(Te, Sb)-O-x. *Top. Catal.* **2003**, *23*, 5–22.
28. Grasselli, R. K. Selectivity Issues in (Amm)oxidation Catalysis. *Catal. Today* **2005**, *99*, 23–31.
29. Baca, M.; Aouine, M.; Dubois, J. L.; Millet, J. M. M. Synergetic Effect Between Phases in MoVTe(Sb)NbO Catalysts Used for the Oxidation of Propane into Acrylic Acid. *J. Catal.* **2005**, *233*, 234–241.
30. Korovchenko, P.; Guliants, V. V.; Guerrero-Perez, M. O., Thermal Transformation of the Mo-V-Te-O M1 to M2 Phases: Synthesis, Structural Characteristics and Catalytic Performance in Propane Ammoxidation. *Abstr. Pap. Am. Chem. Soc.* **2007**, *233*.
31. Korovchenko, P.; Guliants, V. V., On Cooperation of the Mo-V-Te-Nb-O M1 and M2 phases in Propane Ammoxidation to Acrylonitrile. *Abstr. Pap. Am. Chem. Soc.* **2007**, *233*.
32. Kolen'ko, Y. V.; Zhang, W.; d'Alnoncourt, R. N.; Girgsdies, F.; Hansen, T. W.; Wolfram, T.; Schlogl, R.; Trunschke, A. Synthesis of MoVTeNb Oxide Catalysts with Tunable Particle Dimensions. *ChemCatChem* **2011**, *3*, 1597–1606.
33. Pyrz, W. D.; Blom, D. A.; Sadakane, M.; Kodato, K.; Ueda, W.; Vogt, T.; Buttrey, D. J. Atomic-Level Imaging of Mo-V-O Complex Oxide Phase Intergrowth, Grain Boundaries, and Defects Using HAADF-STEM. *Proc. Natl. Acad. Sci. U.S.A.* **2010**, *107*, 6152–6157.
34. Yu, J. J.; Woo, J.; Borisevich, A.; Xu, Y.; Guliants, V. V. A Combined HAADF STEM and Density Functional Theory Study of Tantalum and Niobium Locations in the Mo-V-Te−Ta(Nb)-O M1 Phases. *Catal. Commun.* **2012**, *29*, 68–72.
35. Blom, D. A.; Li, X.; Mitra, S.; Vogt, T.; Buttrey, D. J. STEM HAADF Image Simulation of the Orthorhombic M1 Phase in the Mo-V-Nb-Te-O Propane Oxidation Catalyst. *ChemCatChem* **2011**, *3*, 1028–1033.
36. Sadakane, M.; Endo, K.; Kodato, K.; Ishikawa, S.; Murayama, T.; Ueda, W. Assembly of a Pentagonal Polyoxomolybdate Building Block, [Mo6O21](6-), into Crystalline MoV Oxides. *Eur. J. Inorg. Chem.* **2013**, 1731–1736.
37. Sadakane, M.; Ueda, W. Building Block Synthesis of Crystalline Mo-V-based Oxides: Selective Oxidation Catalysts. *J. Jpn. Pet. Inst.* **2012**, *55*, 229–235.
38. Korovchenko, P.; Shiju, N. R.; Dozier, A. K.; Graham, U. M.; Guerrero-Perez, M. O.; Guliants, V. V. M1 to M2 Phase Transformation and Phase Cooperation in Bulk Mixed Metal Mo-V-M-O (M=Te, Nb) Catalysts for Selective Ammoxidation of Propane. *Top. Catal.* **2008**, *50*, 43–51.
39. Shiju, N. R.; Liang, X.; Weimer, A. W.; Liang, C.; Dai, S.; Guliants, V. V. The Role of Surface Basal Planes of Layered Mixed Metal Oxides in Selective Transformation of Lower Alkanes: Propane Ammoxidation over Surface ab Planes of Mo-V-Te-Nb-O M1 Phase. *J. Am. Chem. Soc.* **2008**, *130*, 5850–5851.
40. Belianinov, A.; He, Q.; Jesse, S.; Borisevich, A.; Kallinin, S. V., Local Crystallography: Phases, Symmetries, and Defects from Bottom Up. *Nat. Comm.*, Submitted for publication.
41. Watanabe, N.; Ueda, W. Comparative Study on the Catalytic Performance of Single-Phase Mo-V-O-based Metal Oxide Catalysts in Propane Ammoxidation to Acrylonitrile. *Ind. Eng. Chem. Res.* **2006**, *45*, 607–614.
42. Nguyen, T. T.; Deniau, B.; Baca, M.; Millet, J. M. M. Synthesis and Monitoring of MoVSbNbO Oxidation Catalysts Using V K and Sb L-1-Edge Xanes Spectroscopy. *Top. Catal.* **2011**, *54*, 650–658.